



## Investigation of the Al–Ti–Pt alloy system at 1100 °C

O.V. Zaikina<sup>a,\*</sup>, V.G. Khorujaya<sup>a</sup>, D. Pavlyuchkov<sup>a</sup>, B. Grushko<sup>b</sup>, T.Ya. Velikanova<sup>a</sup>

<sup>a</sup> I.N. Frantsevich Institute for Problems of Materials Science, 03680, Kyiv-142, Ukraine

<sup>b</sup> PGI-5, Forschungszentrum Jülich, D-52425 Jülich, Germany

### ARTICLE INFO

#### Article history:

Received 21 March 2011

Received in revised form 19 April 2011

Accepted 21 April 2011

Available online 28 April 2011

#### Keywords:

Titanium aluminides

Phase diagrams

### ABSTRACT

The 1100 °C isothermal section of the Al–Ti–Pt system was experimentally studied in the compositional region below 50 at.% Pt. Most of the binary Al–Ti and Al–Pt intermetallics dissolve about 1.5–3.5 at.% of the third element. Only TiAl and Ti<sub>3</sub>Al contain up to ~5.5 at.% Pt and Al<sub>2</sub>Pt ~13 at.% Ti. The Ti<sub>3</sub>Pt, Ti<sub>3</sub>Pt<sub>4</sub> and TiPt phases extend up to 7.5, 9 and 30 at.% Al, respectively. The homogeneity range of the ternary phase  $\tau_1$  extends from Al<sub>63.3</sub>Ti<sub>30.6</sub>Pt<sub>6.1</sub> to Al<sub>69.0</sub>Ti<sub>24.2</sub>Pt<sub>6.6</sub> and that of  $\tau_2$  from Al<sub>44.1</sub>Ti<sub>34.0</sub>Pt<sub>21.9</sub> to Al<sub>55.1</sub>Ti<sub>20.9</sub>Pt<sub>24.0</sub>. The  $\tau_3$ -phase is formed in the compositional region from Al<sub>37</sub>Ti<sub>37.5</sub>Pt<sub>25.5</sub> to Al<sub>42</sub>Ti<sub>32</sub>Pt<sub>26</sub>. Only the Nb(Ir,Al)<sub>2</sub>-type structure of the latter was revealed. The  $\tau_4$ -phase exists between Al<sub>31.3</sub>Ti<sub>33.7</sub>Pt<sub>35</sub> and Al<sub>36.6</sub>Ti<sub>29.4</sub>Pt<sub>34</sub> while the  $\tau_5$ -phase exists between Al<sub>12.9</sub>Ti<sub>58.9</sub>Pt<sub>28.2</sub> and Al<sub>27.3</sub>Ti<sub>57.3</sub>Pt<sub>15.4</sub>. Apart from these previously reported phases, five new ternary compounds designated  $\tau_6$  to  $\tau_{10}$  were revealed. The  $\tau_6$ -phase exists between the Al<sub>25.5</sub>Ti<sub>54.2</sub>Pt<sub>20.3</sub> and the Al<sub>30</sub>Ti<sub>54</sub>Pt<sub>16</sub> compositions, and probably has a primitive cubic structure with  $a = 0.68477(6)$  nm. The  $\tau_7$ -phase was found to be formed around the Al<sub>12</sub>Ti<sub>51</sub>Pt<sub>37</sub> composition,  $\tau_8$ ,  $\tau_9$  and  $\tau_{10}$ -phases exist in the compositional ranges of Al<sub>28.5</sub>Ti<sub>55</sub>Pt<sub>27.5</sub> to Al<sub>33.7</sub>Ti<sub>40</sub>Pt<sub>26.3</sub>, Al<sub>34.5</sub>Ti<sub>48</sub>Pt<sub>17.5</sub> to Al<sub>38</sub>Ti<sub>44</sub>Pt<sub>18</sub> and Al<sub>52.6</sub>Ti<sub>44.3</sub>Pt<sub>23.1</sub> to Al<sub>37.4</sub>Ti<sub>41</sub>Pt<sub>21.6</sub>, respectively.

© 2011 Elsevier B.V. All rights reserved.

### 1. Introduction

The Al–Ti–Pt alloy system was experimentally studied in Refs. [1,2] at 950 °C in a compositional region adjacent to the Al–Ti terminal. Several contributions were also devoted to individual ternary Al–Ti–Pt phases [2–4]. This alloy system is related to the Al–Ti–Pd alloy system, also studied in Refs. [1,2] at 950 °C and more recently in Ref. [5] at 930 and 1100 °C.

Five ternary phases designated  $\tau_1$  to  $\tau_5$  were reported in Refs. [1–5] (see Table 1 for structural details). The  $\tau_1$ -phase and  $\tau_2$ -phase were found to be formed around the Al<sub>67</sub>Ti<sub>26</sub>Pt<sub>7</sub> and Al<sub>50</sub>Ti<sub>25</sub>Pt<sub>25</sub> compositions, respectively. In Ref. [1] the  $\tau_3$ -phase was associated with the Al<sub>42</sub>Ti<sub>44</sub>Pt<sub>14</sub> composition and in Ref. [2] with the Al<sub>43.2</sub>Ti<sub>37.8</sub>Pt<sub>19</sub> composition. The structural variant of this phase designated  $\tau'_3$  in the following was found to exist around 25 at.% Pt and 33.5–36 at.% Ti [2]. The  $\tau_4$ -phase is formed around the equiatomic composition AlTiPt, while the  $\tau_5$ -phase is formed in a compositional range between Al<sub>14</sub>Ti<sub>58</sub>Pt<sub>28</sub> and Al<sub>21</sub>Ti<sub>63</sub>Pt<sub>16</sub>. The solubility of Pt in binary titanium aluminides was found to be in the order of 2.5 at.%.

The phase equilibria presented in Refs. [1,2] are quite schematic and some details are controversial. Even binary boundary alloy systems Al–Pt, Al–Ti and Ti–Pt are still insufficiently well established. In the present work the Al–Ti–Pt phase diagram was studied at 1100 °C in the compositional region below 50 at.% Pt. We selected the temperature higher than that applied in Refs. [1,2] in order to improve the equilibration of the studied alloys. The information on the Al–Pt phase diagram is taken from Refs. [6,7] and on the Ti–Pt phase diagram from Refs. [8–10]. The extensively studied Al–Ti constitutional diagram is still under discussion (see Refs. [11–13] and references therein). As mentioned in Ref. [5] and also applicable here, both diagrams in Refs. [12,13] are consistent in the temperature range relevant to our study. The corresponding data are accepted in the following.

The constitutions of the Al–Ti–Pt and Al–Ti–Pd alloy systems will be compared.

### 2. Experimental

The starting materials were Al of 99.995 mass%, Ti of 99.98 mass% and Pt of 99.8 mass% purity. Ternary alloys (2.5–3 g) of more than 60 compositions were prepared by either arc melting or levitation inductive melting under an argon atmosphere. They were subsequently annealed under an argon atmosphere at 1100 °C for 72–209 h and water quenched.

The alloys were studied by scanning electron microscopy (SEM) and powder X-ray diffraction (XRD). The compositions of the phases were determined in SEM by energy dispersive X-ray analysis (EDX) on polished unetched cross sections. XRD was

\* Corresponding author. Tel.: +38 044 424 3090; fax: +38 044 424 21 31.

E-mail address: [alex.zaikina@googlegmail.com](mailto:alex.zaikina@googlegmail.com) (O.V. Zaikina).

**Table 1**  
Crystallographic data of the Al–Ti–Pt phases in the studied compositional and temperature ranges. The literature data are given with the corresponding references.

Phase	Space group	Prototype	Lattice parameters, nm			Comment
			<i>a</i>	<i>b</i>	<i>c</i>	
h-TiPt ( $\beta$ )	$Pm\bar{3}m$	CsCl	0.3192	–	–	[15]
l-TiPt	$Pmma$	AuCd	0.455	0.273	0.479	[15]
			0.4592	0.2761	0.4838	[16]
Ti <sub>3</sub> Pt	$Pm\bar{3}n$	Cr <sub>3</sub> Si	0.50327	–	–	[17]
			0.5030	–	–	[18]
Ti <sub>4</sub> Pt <sub>3</sub>	Unknown	–	–	–	–	[10]
$\beta$ -AlPt	$Pm\bar{3}m$	CsCl	0.3125	–	–	[19]
$\alpha$ -AlPt	$P2_13$	FeSi	0.4864	–	–	[20]
Al <sub>3</sub> Pt <sub>2</sub>	$P3m1$	Al <sub>3</sub> Ni <sub>2</sub>	0.4204	–	0.5171	[21]
Al <sub>2</sub> Pt	$Fm\bar{3}m$	CaF <sub>2</sub>	0.5910	–	–	[21] Al <sub>67</sub> Pt <sub>33</sub>
			0.5920	–	–	[21] Al <sub>68</sub> Pt <sub>32</sub>
Al <sub>21</sub> Pt <sub>8</sub>	$I4_1/a$	Al <sub>21</sub> Pt <sub>8</sub>	1.2964	–	1.0684	[21]
$\alpha$	$P6_3/mmc$	Mg	0.2951	–	0.4684	[22]
$\alpha_2$	$P6_3/mmc$	Ni <sub>3</sub> Sn	0.5775	–	0.4655	[23]
$\gamma$	$P4/mmm$	AuCu	0.4001	–	0.4071	[23]
$\eta$	$I4_1/amd$	HfGa <sub>2</sub>	0.3976	–	2.436	[23]
$\zeta$	$P4/mmm$	Ti <sub>2</sub> Al <sub>5</sub>	0.39053	–	2.91963	[24]
$\varepsilon$	$I4/mmm$	TiAl <sub>3</sub>	0.3846	–	0.8594	[23]
$\tau_1$	$Fm\bar{3}m$	Cu	0.39577(1)	–	–	[1], 950 °C, Al <sub>65</sub> Ti <sub>25</sub> Pt <sub>10</sub>
	$Pm\bar{3}m$	AuCu <sub>3</sub>	0.396245(3)	–	–	[3], 950 °C, Al <sub>68</sub> Ti <sub>26</sub> Pt <sub>6</sub>
$\tau_2$	$Fm\bar{3}m$	Th <sub>6</sub> Mn <sub>23+1</sub>	1.21921(1)	–	–	[1], 950 °C, Al <sub>50</sub> Ti <sub>25</sub> Pt <sub>25</sub>
			1.22315(5)	–	–	[3], as-cast, Al <sub>50</sub> Ti <sub>25</sub> Pt <sub>25</sub>
$\tau_3$	$P6_3/mmc$	MgZn <sub>2</sub>	0.51309(1)	–	0.82691(1)	[1], 950 °C, Al <sub>42.3</sub> Ti <sub>44.1</sub> Pt <sub>13.6</sub>
$\tau'_3$	$P6_3/mcm$	Nb(Ir,Al) <sub>2</sub>	0.89014(3)	–	0.82019(3)	[2], as-cast, Al <sub>39.6</sub> Ti <sub>36.0</sub> Pt <sub>24.4</sub>
			0.88994(4)	–	0.81974(3)	[2] 950 °C, Al <sub>40.0</sub> Ti <sub>34.9</sub> Pt <sub>25.1</sub>
$\tau_4$	$P6_3/mmc$	ZrBeSi	0.43908(9)	–	0.54823(10)	[4], 1100 °C, Al <sub>33.4</sub> Ti <sub>33.3</sub> Pt <sub>33.3</sub>
			0.43964(2)	–	0.54868(3)	[2], 950 °C, Al <sub>33.4</sub> Ti <sub>33.3</sub> Pt <sub>33.3</sub>
$\tau_5$	$P4_2nm$ or $P4n2$ or $P4_2/mnm$	–	0.97019(20)	–	0.50231(13)	[4], 1100 °C, Al <sub>15</sub> Ti <sub>60</sub> Pt <sub>25</sub>
$\tau_6$	Cubic	–	0.68477(6)	–	–	this work
$\tau_7$	Unknown	Unknown	?	–	–	this work
$\tau_8$	Unknown	Unknown	?	–	–	this work
$\tau_9$	Unknown	Unknown	?	–	–	this work
$\tau_{10}$	Unknown	Unknown	?	–	–	this work

carried out in transmission mode using Cu K $\alpha_1$  radiation and image plate detector ( $2\theta$  range: 5–120°).

### 3. Results and discussion

#### 3.1. Binary phases

According to Ref. [8], at 1100 °C  $\beta$ -Ti can dissolve up to 10 at.% Pt and the high-Ti part of the Ti–Pt alloy system also contains intermetallic phases Ti<sub>3</sub>Pt and h-TiPt (see Table 1) exhibiting some compositional ranges. One more phase of unknown structure designated Ti<sub>4</sub>Pt<sub>3</sub> was reported in Ref. [9]. It was found to exist between 41.7 and 43.4 at.% Ti below 1205 °C. The temperature of the transition between high-temperature h-TiPt and low-temperature l-TiPt varies between 980 and 1050 °C depending on the composition [8–10], i.e. not much below the temperature of 1100 °C applied for our ternary samples. Powder XRD analysis of the relevant ternary samples annealed at and quenched from 1100 °C indicated the presence of some l-TiPt together with h-TiPt. It can be explained rather by transformation by cooling than by increase of the transition temperature between these phases due to the addition of Al.

In our experiments a sample of composition Ti<sub>57.2</sub>Pt<sub>42.8</sub> annealed at 1100 °C exhibited a major phase associated with Ti<sub>4</sub>Pt<sub>3</sub> of Ref. [9]. Powder XRD pattern obtained from this sample was qualitatively similar to that in Fig. 6 of Ref. [9]. Investigation of the samples by transmission electron microscopy revealed strongly faulted microstructure [14]. This did not allow the structural analysis of this phase also by electron diffraction.

**Table 2**

Diffraction data of the  $\tau_6$ -phase (Cubic,  $a=0.68477(6)$  nm, average  $\Delta 2\theta=0.020^\circ$ , maximum  $\Delta 2\theta=0.134^\circ$ , figure of merit  $F(30)=49.9$ . From the total of 50 collected reflections, those below 3% are not included).

No.	<i>h</i>	<i>k</i>	<i>l</i>	$d_{obs}$	$d_{calc}$	$I/I_0$
1	1	1	0	0.48506	0.48421	29
2	1	1	1	0.39589	0.39535	50
3	2	0	0	0.34259	0.34239	25
4	2	1	0	0.30625	0.30624	39
5	2	1	1	0.27969	0.27956	12
6	2	2	0	0.24217	0.24210	9
7	3	0	0	0.22828	0.22826	100
8	3	1	0	0.21652	0.21654	65
9	3	1	1	0.20643	0.20647	23
10	2	2	2	0.19773	0.19768	3
11	3	2	0	0.18989	0.18992	11
12	3	2	1	0.18300	0.18301	36
13	4	1	0	0.16610	0.16608	19
14	3	3	0	0.16139	0.16140	5
15	3	3	1	0.15709	0.15710	5
16	4	2	0	0.15308	0.15312	3
17	4	2	1	0.14945	0.14943	6
18	4	2	2	0.13974	0.13978	6
19	5	0	0	0.13694	0.13695	6
20	5	1	0	0.13429	0.13429	31
21	5	1	1	0.13178	0.13178	9
22	5	2	0	0.12716	0.12716	20
23	5	2	1	0.12501	0.12502	7
24	5	3	1	0.11576	0.11575	4
25	6	0	0	0.11413	0.11413	9
26	5	4	0	0.10694	0.10694	6
27	5	4	1	0.10565	0.10566	3
28	5	3	3	0.10442	0.10443	3
29	6	3	0	0.10206	0.10208	4
30	6	3	1	0.10096	0.10096	3
31	7	0	0	0.09780	0.09782	3

The  $\text{Ti}_3\text{Pt}$  and  $\text{Ti}_3\text{Pt}_4$  phases dissolve 7.5 and 9 at.% Al, respectively, while  $\text{TiPt}$  dissolves up to 30 at.% Al.

At the studied temperature the relevant part of the Al–Pt alloy system contains the congruent  $\text{AlPt}$  and  $\text{Al}_3\text{Pt}_2$  phases and peritectically forming  $\text{Al}_2\text{Pt}$  and  $\text{Al}_{21}\text{Pt}_8$  phases [6,7] (see Table 1). Only in  $\text{Al}_2\text{Pt}$  does the solubility of Ti reach 13 at.%; the other Al–Pt phases were found to dissolve no more than 3.5 at.% Ti.

At 1100 °C the Al–Ti system contains the terminal solid solutions  $\alpha_{\text{Ti}}$  and  $\beta_{\text{Ti}}$ , and intermediate phases  $\alpha_2$  ( $\text{AlTi}_3$ ),  $\gamma$  ( $\text{AlTi}$ ),  $\eta$  ( $\text{Al}_2\text{Ti}$ ),  $\zeta$  ( $\text{Al}_5\text{Ti}_2$ ) and high-temperature  $\varepsilon$  ( $\text{Al}_3\text{Ti}$ ) (see Table 1 for crystallographic data). The  $\beta_{\text{Ti}}$ -phase extends up to ~20 at.% Al,  $\alpha_2$  between 27 and 38 at.% Al,  $\gamma$  between 47 and 61 at.% Al. The other phases exhibit narrower compositional regions. The solubility of Pt in the Al–Ti intermetallics is quite low. The  $\text{TiAl}_3$ ,  $\text{Ti}_2\text{Al}_5$  and  $\text{TiAl}_2$  phases dissolve up to 1.5 at.% Pt, whereas  $\text{TiAl}$  and  $\text{Ti}_3\text{Al}$  contain up to ~5.5 at.% Pt.

The observed propagation of the binary phases into the ternary space is exhibited in the isothermal section (see below).

### 3.2. Ternary phases

Apart from the ternary phases mentioned in the Introduction, our study revealed five more ternary phases designated  $\tau_6$ , to  $\tau_{10}$ . Their compositions were determined in two-phase and three-phase equilibrated samples and new samples were produced in order to reduce the volume fraction of impurity phases. The powder XRD patterns of the essentially major  $\tau_6$ ,  $\tau_7$ ,  $\tau_8$  and  $\tau_9$  phases selected after SEM/EDX examinations are shown in Fig. 1 together with those of the  $\tau_1$  to  $\tau_5$ . The XRD diffraction pattern of  $\tau_{10}$  has not been obtained due to absence of a sample contained major fraction of this phase. The diffraction pattern of the  $\tau_6$ -phase could be indexed for a primitive cubic structure with the lattice parameter  $a = 0.68477(6)$  nm (see Table 2). The possible lattice constants of the  $\tau_7$ ,  $\tau_8$ ,  $\tau_9$  and  $\tau_{10}$ -phases exhibiting complicated diffraction patterns were not determined.

According to our measurements, the  $\tau_1$ -phase exists between the  $\text{Al}_{63.3}\text{Ti}_{30.6}\text{Pt}_{6.1}$  and the  $\text{Al}_{69.0}\text{Ti}_{24.2}\text{Pt}_{6.6}$  compositions, the  $\tau_2$ -phase between the  $\text{Al}_{44.1}\text{Ti}_{34.0}\text{Pt}_{21.9}$  and the  $\text{Al}_{55.1}\text{Ti}_{20.9}\text{Pt}_{24.0}$  compositions and the  $\tau_3$ -phase in a small compositional region from  $\text{Al}_{37}\text{Ti}_{37.5}\text{Pt}_{25.5}$  to  $\text{Al}_{42}\text{Ti}_{32}\text{Pt}_{26}$ . Only the  $\tau_3'$  superstructure (see Table 1) was revealed in our experiments at 1100 °C.

The compositional regions between  $\text{Al}_{31.3}\text{Ti}_{33.7}\text{Pt}_{35}$  and  $\text{Al}_{36.6}\text{Ti}_{29.4}\text{Pt}_{34}$  were determined for the  $\tau_4$ -phase and from  $\text{Al}_{12.9}\text{Ti}_{58.9}\text{Pt}_{28.2}$  to  $\text{Al}_{27.3}\text{Ti}_{57.3}\text{Pt}_{15.4}$  for the  $\tau_5$ -phase. The  $\tau_6$ -phase exists between the  $\text{Al}_{25.5}\text{Ti}_{54.2}\text{Pt}_{20.3}$  and the  $\text{Al}_{30}\text{Ti}_{54}\text{Pt}_{16}$  compositions. The  $\tau_7$ -phase occupies a small range around the  $\text{Al}_{12}\text{Ti}_{51}\text{Pt}_{37}$  composition, while the  $\tau_8$ ,  $\tau_9$  and  $\tau_{10}$ -phases are formed in the compositional ranges of  $\text{Al}_{28.5}\text{Ti}_{55}\text{Pt}_{27.5}$  to  $\text{Al}_{33.7}\text{Ti}_{40}\text{Pt}_{26.3}$ ,  $\text{Al}_{34.5}\text{Ti}_{48}\text{Pt}_{17.5}$  to  $\text{Al}_{38}\text{Ti}_{44}\text{Pt}_{18}$  and  $\text{Al}_{32.6}\text{Ti}_{44.3}\text{Pt}_{23.1}$  to  $\text{Al}_{37.4}\text{Ti}_{41}\text{Pt}_{21.6}$ , respectively.

The absence of the  $\tau_7$ -phase in the as-cast samples and the existence of the  $\tau_7 + \text{Ti}_3\text{Pt}_5 + \tau_4$ ,  $\tau_7 + \tau_4 + \text{Ti}_3\text{Pt}_5$  and  $\text{Ti}_3\text{Pt} + \tau_7 + \tau_4$  equilibria at 1100 °C probably indicate a peritectoid character of its formation at temperatures above 1100 °C.

### 3.3. Isothermal section 1100 °C

The partial 1100 °C isothermal section of the Al–Ti–Pt alloy system determined in our work is shown in Fig. 2. The equiatomic  $\tau_4$ -phase is in equilibrium with the  $\tau_2$ ,  $\tau_3$ ,  $\tau_5$ ,  $\tau_7$  and  $\tau_8$ -phases and the ternary extensions of the binary

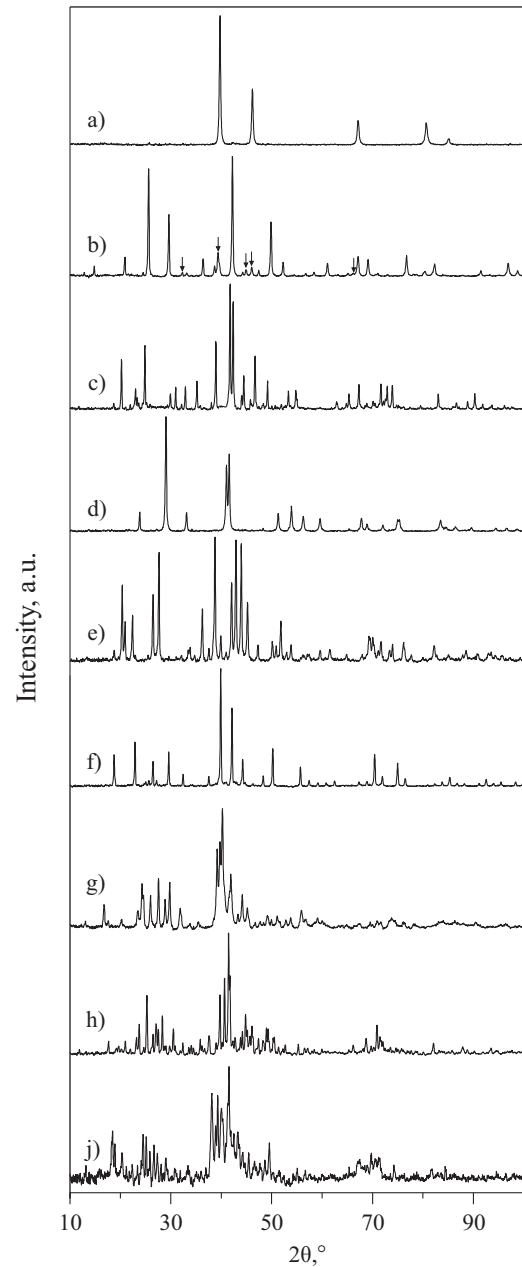


**Fig. 1.** Powder XRD patterns of the alloys annealed at 1100 °C (CuK $\alpha_1$  radiation, the corresponding phases are mentioned in brackets): (a)  $\text{Al}_{67.4}\text{Ti}_{24.8}\text{Pt}_{7.8}$  ( $\tau_1 + \text{Al}_2\text{Pt}^*$ ), (b)  $\text{Al}_{56.4}\text{Ti}_{30}\text{Pt}_{13.6}$  ( $\tau_2$  and some  $\gamma$  whose reflections are marked by arrows), (c)  $\text{Al}_{35.8}\text{Ti}_{37.8}\text{Pt}_{26.4}$  ( $\tau_3 + \tau_8^*$ ), (d)  $\text{Al}_{34.7}\text{Ti}_{29.6}\text{Pt}_{35.7}$  ( $\tau_4$ ), (e)  $\text{Al}_{16.9}\text{Ti}_{57.6}\text{Pt}_{25.5}$  ( $\tau_5 + \tau_6^* + \tau_8^*$ ), (f)  $\text{Al}_{30}\text{Ti}_{50.8}\text{Pt}_{19.2}$  ( $\tau_6 + \tau_{10}^*$ ), (g)  $\text{Al}_{13.9}\text{Ti}_{49.4}\text{Pt}_{36.7}$  ( $\tau_7 + \tau_4^* + \text{Ti}_4\text{Pt}_3^*$ ), (h)  $\text{Al}_{32.1}\text{Ti}_{43.2}\text{Pt}_{24.7}$  ( $\tau_8 + \tau_{10}^*$ ) and (j)  $\text{Al}_{38.1}\text{Ti}_{44.1}\text{Pt}_{17.8}$  ( $\tau_9 + \tau_{10}^*$ ). The additional phases marked by (\*) were observed by SEM in very small amounts whose contributions to the powder XRD patterns were essentially minor.

phases  $\text{Ti}_4\text{Pt}_3$ ,  $\text{TiPt}$ ,  $\text{Al}_3\text{Pt}_2$  and  $\text{Al}_2\text{Pt}$ . The three-phase equilibria  $\tau_4 + \text{TiPt} + \text{Al}_3\text{Pt}_2$ ,  $\tau_4 + \text{Al}_3\text{Pt}_2 + \text{Al}_2\text{Pt}$ ,  $\tau_4 + \text{Al}_2\text{Pt} + \tau_2$ ,  $\tau_2 + \tau_3 + \tau_4$ ,  $\tau_3 + \tau_4 + \tau_8$ ,  $\tau_4 + \tau_5 + \tau_8$ ,  $\tau_4 + \text{Ti}_3\text{Pt} + \tau_5$ ,  $\tau_4 + \text{Ti}_3\text{Pt} + \tau_7$ ,  $\tau_4 + \text{Ti}_4\text{Pt}_3 + \tau_7$  and  $\tau_4 + \text{Ti}_4\text{Pt}_3 + \text{TiPt}$  were established. Ternary phases, excluding  $\tau_3$ ,  $\tau_7$ ,  $\tau_8$  and  $\tau_{10}$ , coexist in equilibria with the Al–Ti binaries. Thus, the  $\tau_5 + \text{Ti}_3\text{Pt} + \alpha$ ,  $\tau_5 + \alpha + \alpha_2$ ,  $\tau_5 + \tau_6 + \alpha_2$ ,  $\tau_6 + \tau_9 + \alpha_2$ ,  $\tau_9 + \alpha_2 + \gamma$ ,  $\tau_9 + \tau_2 + \gamma$ ,  $\tau_1 + \tau_2 + \gamma$ ,  $\tau_1 + \text{Al}_2\text{Pt} + \varepsilon$  equilibria were revealed. The equilibrium of the  $\tau_1$ -phase with  $\eta$  and  $\zeta$  phase was concluded on the basis of the investigation of two-

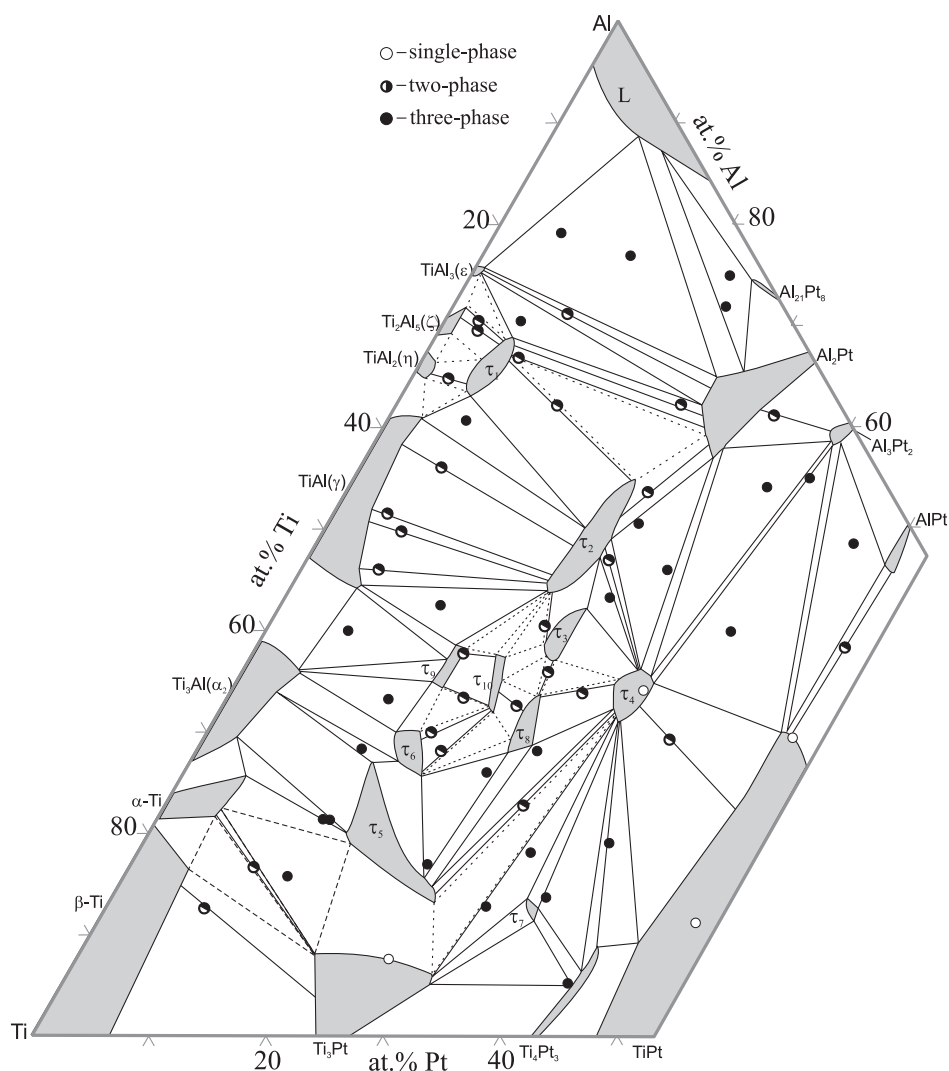


**Fig. 2.** Partial 1100 °C isothermal section of Al–Ti–Pt. The liquid is designated L. The compositions of the studied samples are shown by symbols explained in the drawing. Provisional tie-lines are shown by broken lines.

phase and neighboring three-phase samples. Moreover, the  $\tau_2$ ,  $\tau_3$ ,  $\tau_6$ ,  $\tau_8$ ,  $\tau_9$  and  $\tau_{10}$ -phases coexist in equilibria with each other.

Three-phase equilibria involving the liquid phase include  $\varepsilon + \text{Al}_2\text{Pt} + \text{L}$  and  $\text{Al}_2\text{Pt} + \text{Al}_{21}\text{Pt}_8 + \text{L}$ .

The compositional regions of the ternary phases determined in Refs. [1,2] are compared with our findings in Fig. 3. The results in Ref. [2] are in fair agreement with our isothermal section, while the composition of the  $\tau_3$ -phase in Ref. [1] does not correspond to any single-phase region in either Ref. [2] or our work. Subsequently, the  $\tau_2 + \tau_3 + \gamma$  and  $\tau_3 + \alpha_2 + \gamma$  equilibria reported in Ref. [1] were not confirmed and the  $\tau_3$  phase was not found in equilibrium with the binary Al–Ti phases.

### 3.4. Comparison with Al–Ti–Pd

The compositional regions of the phases in the Al–Ti–Pt alloy system are compared in Fig. 4 with those determined in Ref. [5] in the Al–Ti–Pd alloy system at the same 1100 °C. Also the composition of the Al–Ti–Pd  $\tau_2$ -phase forming somewhat below this

temperature is added. The solubility of Pt and Pd in the Al–Ti binary phases is comparable. The three ternary compounds revealed in Al–Ti–Pd were also found in Al–Ti–Pt. They are designated by the same names. Their compositional regions are somewhat different (see Fig. 4). Both the  $\text{MgZn}_2$ -type structure of the  $\tau_3$ -phase and the  $\text{Nb}(\text{Ir},\text{Al})_2$ -type superstructure variants (designated  $\tau'_3$ ) were observed in the Al–Ti–Pd alloy system. The  $\text{MgZn}_2$ -type structure, reported in Ref. [1] to be also formed in Al–Ti–Pt at 930 °C, was not observed in our study at 1100 °C nor in Ref. [2] at 930 °C.

The main differences between the constitutions of the Al–Ti–Pd and Al–Ti–Pt alloy systems are due to the differences between the Al–Pd and the Al–Pt binary systems. Instead of a wide continuous region of the  $\beta$  solid solution in the former, the disordered  $\beta_{\text{Ti}}$  solid solution only slightly extends into the ternary compositional region in the latter, and the ordered solid-solution  $\beta$  extends from TiPt as a narrow stripe towards AlPt. In the ternary region corresponding in Al–Ti–Pd to the  $\beta$ -phase numerous ternary phases were revealed in Al–Ti–Pt. In total the number of ternary phases in the Al–Ti–Pt system is much higher than in Al–Ti–Pd.

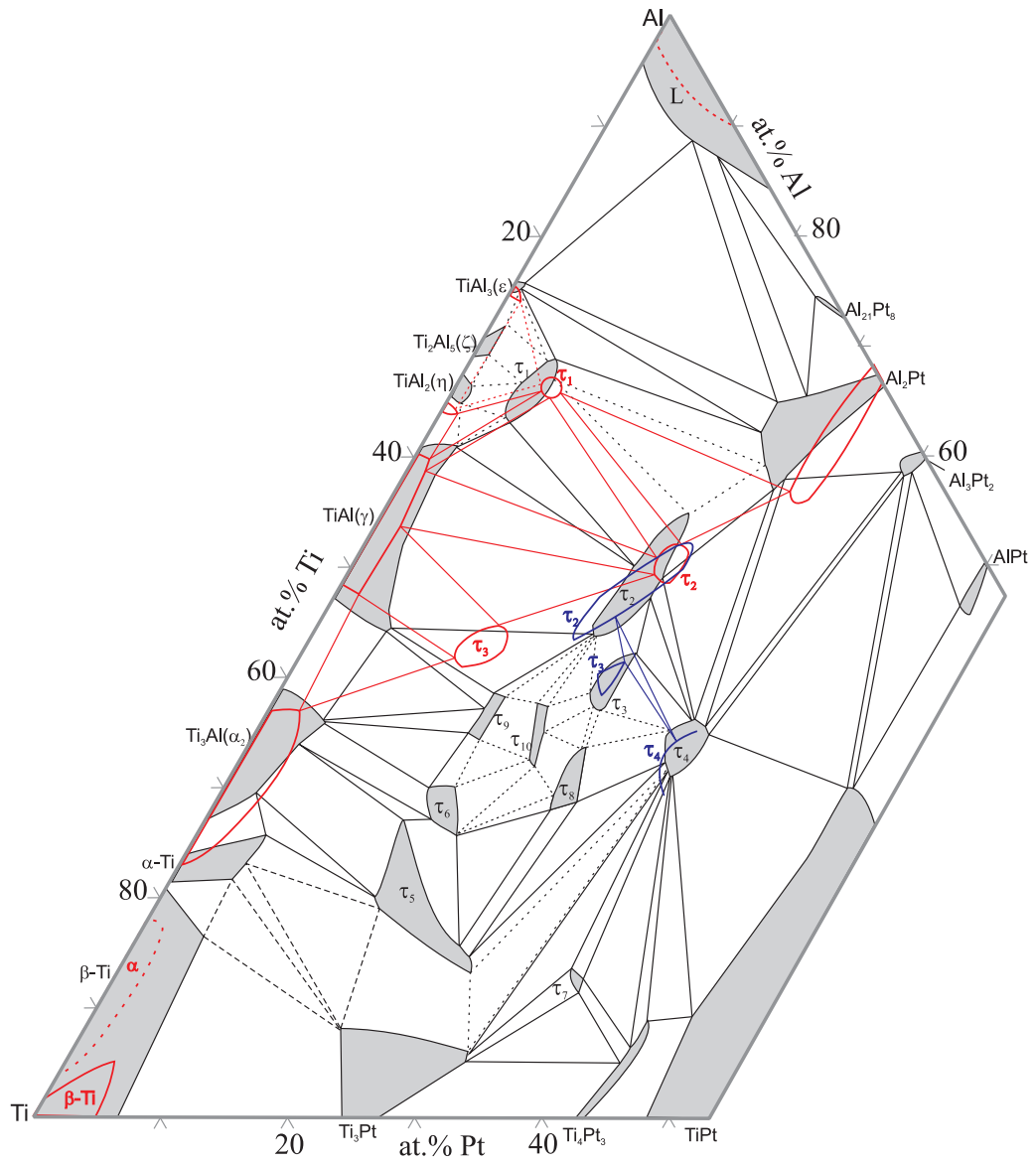


**Fig. 3.** The results of the present study as in Fig. 2 (thin solid lines) compared to those in Ref. [1] (red in the online version) and Ref. [2] (blue in the online version). The literature data correspond to 950 °C.

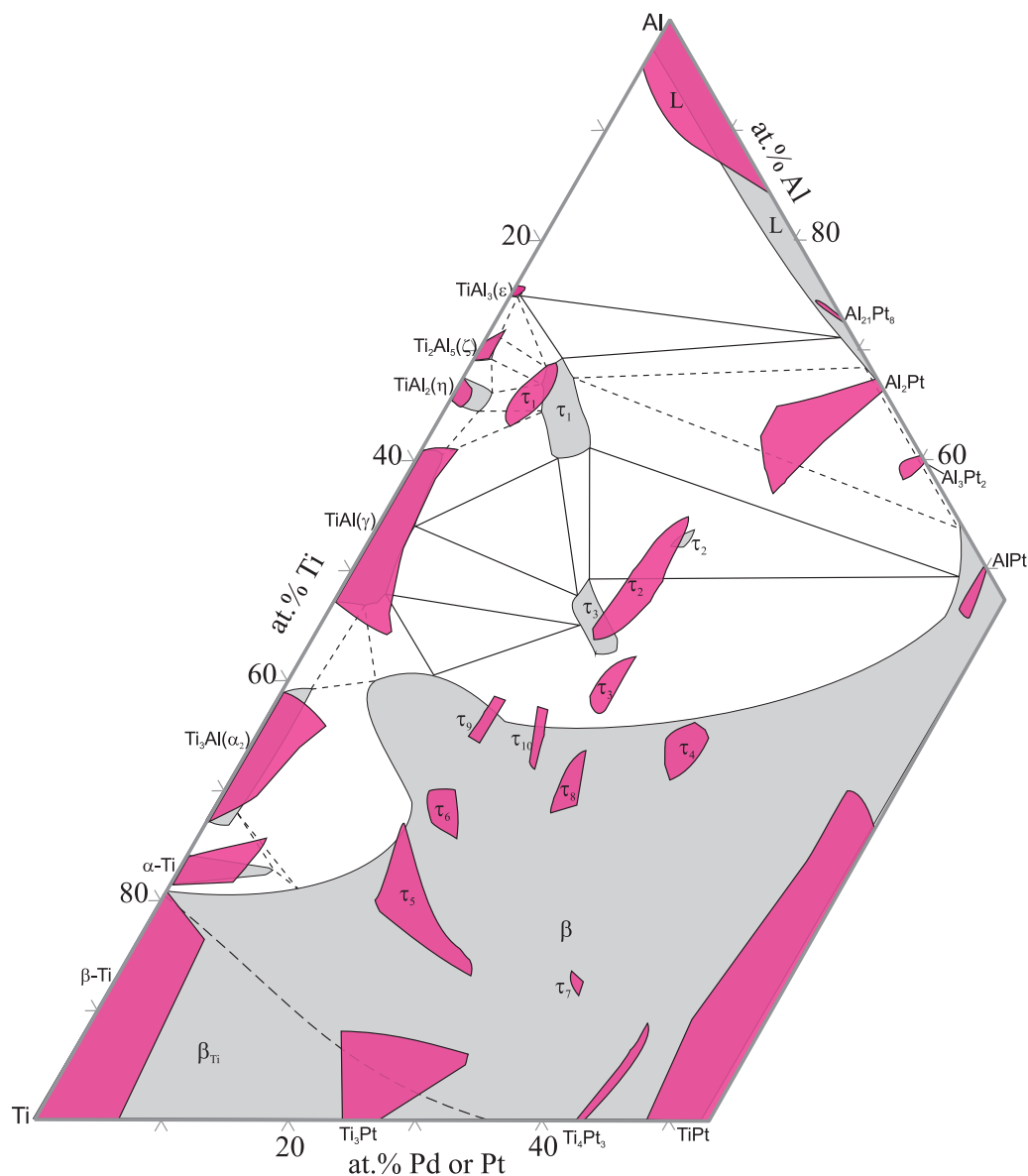


**Fig. 4.** Compositional regions of the phases in Al–Ti–Pt (pink in the online version) compared to those in Al–Ti–Pd [5]. The tie-lines correspond to the equilibrium in Al–Ti–Pd at 1100 °C. The Al–Ti–Pd  $\tau_2$ -phase forming at lower temperatures is also shown.

#### 4. Conclusions

Partial isothermal section of the Al–Ti–Pt phase diagram at 1100 °C was determined in the compositional region below 50 at.% Pt.

Binary Al–Ti phases dissolve from 1.5 to 5.5 at.% Pt. The solubility of Ti in  $\text{Al}_2\text{Pt}$  reaches 13 at.%, and the other Al–Pt phases forming in the studied compositional region dissolve below 3.5 at.% of Ti. The TiPt phase extends up to 30 at.% Al,  $\text{Ti}_3\text{Pt}$  and  $\text{Ti}_3\text{Pt}_4$  up to 7.5 and 9 at.% Al, respectively.

The ternary compounds  $\tau_1$  to  $\tau_5$  earlier reported were confirmed. The  $\text{MgZn}_2$ -type structure associated in the literature with the  $\tau_3$ -phase was not found at 1100 °C, but only its superstructure of the  $\text{Nb}(\text{Ir},\text{Al})_2$  type.

Five regions of the new ternary phases, designated  $\tau_6$  to  $\tau_{10}$  were revealed. The structures of these phases have not yet been determined. The  $\tau_6$ -phase probably has a primitive cubic structure with the lattice parameter  $a = 0.68477$  nm.

#### Acknowledgements

We thank M. Schmidt and B. Jülich for alloy preparation, V. Lenzen and A. Besmehn for XRD measurements and S.B. Mi for transmission electron microscopy examinations. A.Z. and T.V thank Forschungszentrum Jülich for hospitality.

#### References

- [1] J.J. Ding, P. Rogl, B. Chevalier, J. Etourneau, *Intermetallics* 8 (2000) 1377.
- [2] X. Yan, A. Grytsiv, P. Rogl, H. Schmidt, G. Giester, A. Saccone, X.-Q. Chen, *Intermetallics* 17 (2009) 336.
- [3] A. Grytsiv, P. Rogl, H. Schmidt, G. Giester, P. Hundegger, G. Wiesinger, V. Pomjakushin, *Intermetallics* 12 (2004) 563.
- [4] O. Zaikina, V. Khorujaya, D. Pavlyuchkov, T. Velikanova, *Powder Diffr.* 23 (2008) 360.
- [5] O. Zaikina, V. Khorujaya, D. Pavlyuchkov, B. Grushko, T. Velikanova, *J. Alloys Compd.* 509 (2011) 43.
- [6] A.J. McAlister, D.J. Kahan, *Bull. Alloy Phase Diagrams* 7 (1986) 47.
- [7] K. Wu, Z. Jin, *J. Phase Equilib.* 21 (2000) 321.
- [8] J.L. Murray, *Bull. Alloy Phase Diagrams* 3 (1982) 329.

- [9] T. Biggs, L.A. Cornish, M.J. Witcomb, M.B. Cortie, *J. Alloys Compd.* 375 (2004) 120.
- [10] M. Li, W. Han, C. Li, *J. Alloys Compd.* 461 (2008) 189.
- [11] V.T. Witusiewicz, A.A. Bondar, U. Hecht, S. Rex, T.Ya. Velikanova, *J. Alloys Compd.* 465 (2008) 64.
- [12] A. Grytsiv, P. Rogl, H. Schmidt, J. Giester, *J. Phase Equilib.* 24 (2003) 511.
- [13] J.C. Schuster, M.J. Palm, *Phase Equilib. Diffus.* 27 (2006) 255.
- [14] S.B. Mi, personal communication.
- [15] H.C. Donkersloot, J.H.N. Van Vucht, *J. Less-Common Met.* 20 (1970) 83.
- [16] A.E. Dwight, R.A. Conner, J.W. Downey, *Acta Crystallogr.* 18 (1965) 835.
- [17] E.C. van Reuth, R.M. Waterstrat, *Acta Crystallogr. B* 24 (1968) 186.
- [18] A. Junod, R. Flukiger, J. Mueller, *J. Phys. Chem. Solids* 37 (1976) 27.
- [19] S. Bhan, H. Kudielka, *Z. Metallkd.* 69 (1978) 333.
- [20] R. Ferro, R. Capelli, G. Rambaldi, *Atti Accad. Naz. Lincei, Rend. Cl. Sci. Fis. Mat. Nat.* 34 (1963) 45.
- [21] M. Ellner, U. Kattner, B. Predel, *J. Less-Common Met.* 87 (1982) 305.
- [22] R.M. Wood, *Proc. Phys. Soc.* 80 (1962) 783.
- [23] J. Braun, M. Ellner, *J. Alloys Compd.* 309 (2000) 118.
- [24] J.C. Schuster, H. Ipsier, *Z. Metallkd.* 81 (1990) 383.